

## Recovery behavior of tellurium irradiated with 20-MeV electrons and the influence of lattice defects on the transport properties

K.-H. Helmreich\* and G. Landwehr

*Max-Planck-Institut für Festkörperforschung, Hochfeld-Magnetlaboratorium Grenoble, 166 X, F 38042 Grenoble Cedex, France*

K. Keck

*Physikalisches Institut der Universität, 8700 Würzburg, Germany*

(Received 5 May 1980)

The reaction kinetics of the 50-K recovery stage of tellurium irradiated with 20-MeV electrons can be explained by correlated vacancy-interstitial annihilation. Moreover, the influence of the doping on the transport properties of irradiated tellurium crystals was investigated. It turned out that the assumption of a reduction of the dislocation scattering potential by vacancy trapping as proposed in previous papers is insufficient. The experimental findings are comprehensible if screening of the dislocations by free carriers is assumed to be the predominant mechanism. With this model the doping dependence of the mobility in unirradiated tellurium crystals can also be understood.

### I. INTRODUCTION

A considerable amount of work has been devoted to the investigation of the conduction mechanisms in the elemental semiconductor tellurium; nevertheless, our present knowledge is rather incomplete. Part of the problem arises from a number of rather unusual properties of Te. In the past, the preparation of high-quality single crystals of sufficient purity turned out to be difficult. After this problem was solved—it is possible nowadays to pull single crystals with a low-temperature free-carrier concentration of a few  $10^{13} \text{ cm}^{-3}$ —it turned out that dislocations play an important role in the transport properties. Even if tellurium crystals are prepared with extreme care, dislocation densities of the order  $10^4 \text{ cm}^{-2}$  seem unavoidable. An additional complication in low-temperature experiments is accumulation layers of chemical origin at the surface which act as a bypass for a bulk current. Another handicap results from the small energy difference of a few meV between the valence band and the acceptor levels associated with lattice defects in Te.

In order to find out whether the quasimetallic behavior of pure Te at helium temperatures could possibly arise from intrinsic point defects, studies of the influence of 1-MeV electron irradiation on the transport properties were initiated a few years ago.<sup>1</sup> It turned out that the hole density—Te is always *p* type in the extrinsic range—always increases with

the irradiation dose. The investigation of the annealing behavior revealed two striking recovery stages in the carrier isochronals, a very sharp one at 50 K and another around 110 K. Surprisingly enough, the mobility could be substantially improved by electron irradiation.<sup>2</sup> In order to explain this unusual behavior, a mechanism was invoked which explained the increase in the mobility by shielding of built-in dislocations by irradiation-induced vacancies.<sup>3</sup> This model could describe the early findings.<sup>4</sup> When the experiments were, however, extended to plastically deformed samples<sup>5</sup> it was not possible to explain the data with the proposed model. Moreover, difficulties existed in the interpretation of the microscopic nature of the 50-K recovery stage. Also, the shape of the mobility isochronals could not be explained satisfactorily; it was especially not clear why in the 50-K stage the mobility decreases at small doses and increases at high doses.

In order to clarify the situation, irradiation experiments with 20-MeV electrons were performed. The higher electron energy has the advantage that it is possible to achieve a rather homogeneous distribution of the irradiation defects generated in relatively thick samples. The preparation and handling of single-crystal specimens of about  $100 \mu\text{m}$  thickness had caused some problems in the 1-MeV irradiation experiments. Moreover, the availability of very pure Te specimens promised to provide new insights into the transport properties. In order to learn more

about the influence of dislocations, we studied plastically deformed crystals. Another goal of this investigation was to obtain reliable information about the energy levels of the radiation-induced point defects.

In the following, we shall first discuss relevant aspects of lattice defects, particularly the dislocations in Te. Subsequently, we outline the problems associated with the determination of those energy levels which are generated by the irradiation defects.

In Sec. VI we discuss the results for the dependence of the mobility on electron irradiation. The data can be explained if it is assumed that in crystals of very high purity the free holes are located in a disturbed region around the dislocations where the mobility is reduced with respect to the bulk value. Introduction of point defects by irradiation or doping populates the dislocation-free regions of the samples with holes and results in an increase of the effective mobility.

In Sec. VII isochronal annealing data will be presented which were obtained for deformed and undeformed specimens of different doping after irradiations with various doses. Analysis of the first recovery stage suggests a close-pair recombination, whereas the second stage can be understood as an uncorrelated vacancy-interstitial annihilation.

Finally we discuss possible reasons for the existence of deformation-induced acceptor states which do not anneal at room temperature. These states are introduced into the crystal by a well-defined deformation process which should produce  $a$  edge dislocations oriented parallel to the crystallographic  $c$  axis.

## II. LATTICE DEFECTS IN TELLURIUM

The transport properties of pure and slightly doped Te single crystals at low temperatures are influenced quite substantially by the existence of strong accumulation layers at the surface and dislocations and point defects in the bulk. For pure samples the natural surface layers can mask the galvanomagnetic properties of the bulk completely, especially at very low temperatures. Field-effect measurements showed that the influence of the surface can be reduced drastically by employing a new etching process,<sup>6</sup> which means that our samples exhibit essentially bulk properties in the investigated temperature range ( $T \geq 10$  K).

The dislocation density of at least  $10^4$  dislocations per  $\text{cm}^2$  is rather high in Te single crystals compared with the classical semiconductors Si and Ge.

The high dislocation density is caused by the special binding properties in Te (Sec. III). Since crystals with fewer dislocations cannot be produced, many authors studied the influence of the dislocations by increasing the dislocation density deliberately by plastic deformation.<sup>7-15</sup>

The concentration of the holes can be varied by chemical doping (e.g., with antimony), but fluctuations of the dislocation density in different samples may occur because the specimens are extremely susceptible to plastic deformation. Therefore assertions about the influence of the free carriers drawn from measurements on various specimens are clouded with considerable uncertainty. Subsequently it will be shown that the low-temperature irradiation of Te with high-energy electrons is a suitable method of varying the hole density continuously in the same sample.

## III. CRYSTAL AND DISLOCATION STRUCTURE

The lattice of Te can be described as a hexagonal array of parallel helical chains with threefold screw axes. The direction of these helices defines the crystallographic  $c$  axis. Viewed along the  $c$  axis on the crystal, the chains reduce to equilateral triangles (Fig. 1).

Because of the six valence electrons there is a tendency for the elements of group VIb to compose linear structures. Thus at first it was assumed that

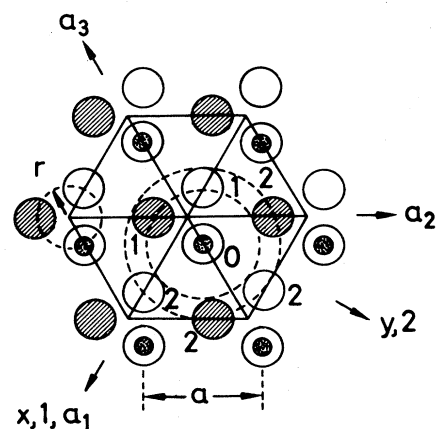


FIG. 1. Projection of the Te lattice in the  $xy$  plane.  $\bigcirc$ , first (fourth) atom in chain.  $\bullet$ , second atom in chain.  $\odot$ , third atom in chain. 1 (2): first (second) nearest neighbor to atom 0.  $a_1$ ,  $a_2$ ,  $a_3$ , and  $c$  are the four hexagonal axes.  $c = 5.95 \text{ \AA}$ ,  $a = 4.45 \text{ \AA}$ ,  $r = 1.19 \text{ \AA}$  (Ref. 16) ( $c$  is the distance between the first and fourth atom in chain).

each atom in the Te lattice is covalently bound to its two next-nearest neighbors within a chain, where there is merely van der Waals attraction between the chains. However this crude model is too simple in the case of Te. As the distance of an atom to the four second-nearest neighbors located in three adjacent chains (Fig. 1) is only 20% higher than the distance to the two next-nearest neighbors within a chain, there is no pure covalent binding within a single chain. Also, the binding between the chains is stronger than the van der Waals attraction alone. In spite of this more complex binding behavior, the bonds inside a chain are strong and directional, whereas the bond between different chains is weaker. The binding energy of the two next-nearest neighbors is about 1.5 times larger than that of the four second-nearest neighbors.<sup>16</sup>

Owing to this peculiar structure, slip should occur on planes parallel to the axes of the chains (prismatic planes) in order to avoid moving dislocations breaking strong bonds within the chains ("covalent bonds").<sup>8</sup> Uniaxial compression experiments show that for homogeneous stress the only glide planes are prismatic planes of the first kind  $\{0110\}$  (cleavage planes) with slip vector (Burgers vector)  $a = \frac{1}{3}\langle 2\bar{1}10 \rangle$  ( $a$  glide) and  $c = \langle 0001 \rangle$  ( $c$  glide). Furthermore, it turns out that the dislocations have a strong tendency to align themselves parallel to the  $c$  axis.<sup>7</sup> This favors the  $a$  edge dislocation and the  $c$  screw dislocation. If only the  $a$  glide system becomes activated, which consists of three subsystems ( $01\bar{1}0$ ,  $2\bar{1}\bar{1}0$ ;  $10\bar{1}0$ ,  $[\bar{1}210]$ ;  $1\bar{1}00$ ,  $[11\bar{2}0]$ ), only  $a$  edge dislocations should be produced. According to Schmid's law<sup>17</sup> pure  $a$  glide should occur if the compression axis is perpendicular to the  $c$  axis ( $a$  deformation). If in this case the angle between the compression axis and the normal vector of one of the  $\{01\bar{1}0\}$  planes is  $0^\circ$  or  $30^\circ$  two of the glide systems should be activated equivalently, but not the third one (duplex  $a$  glide). If the angle is  $15^\circ$ , one glide system is favored (simplex  $a$  glide). This prediction can be experimentally verified by the etch-pit technique<sup>15</sup> because the dislocations have the tendency to build up layers oriented parallel to the activated glide planes.

In order to check the influence of dislocations on the galvanomagnetic properties, it is useful to write down for a homogeneous crystal in thermal equilibrium the relation between the electric field, magnetic field, and current:

$$E_i = \rho_{ik}(\vec{B})j_k \quad (1)$$

The galvanomagnetic transport coefficients  $\rho_{ik}(\vec{B})$

can be expanded in increasing powers of  $B$ :

$$\rho_{ik}(\vec{B}) = \rho_{ik} + \rho_{ikl}B_l + \dots \quad (2)$$

Because the Te lattice belongs to the point group 32 ( $D_3$ ) the resistivity tensor ( $\rho_{ik}$ ) as well as the Hall-effect tensor ( $\rho_{ikl}$ ) have only two independent components, namely  $\rho_{11} = \rho_{\perp}(\vec{j} \perp c)$ ,  $\rho_{33} = \rho_{\parallel}(\vec{j} \parallel c)$  and  $\rho_{132} = R_{\perp}(\vec{B} \perp c)$ ,  $\rho_{123} = R_{\parallel}(\vec{B} \parallel c)$ , respectively. (The indices 1,2,3 stand for the directions of the  $x,y,z$  axes.) It is possible to determine these quantities by measuring samples cut in three special orientations from the crystal (Fig. 2), which leads to three different Hall mobilities:

$$\mu_S^H = R_{\parallel}/\rho_{\perp}, \quad \mu_L^H = R_{\perp}/\rho_{\parallel}, \quad \mu_Q^H = R_{\perp}/\rho_{\perp} \quad (3)$$

For undeformed samples cut from high-quality crystals grown in the  $c$  direction it can be expected that there is a homogeneous distribution of the dislocations with respect to the symmetry operations of the point group 32. Indeed, no anisotropy of the galvanomagnetic quantities can be found for undeformed samples in the  $xy$  plane.<sup>12,15</sup> So we need not take into account new tensor components. In samples that were subjected to an  $a$  deformation at room temperature ( $\Delta l/l$  a few percent, deformation velocity  $v = 2 \times 10^{-4}$  mm/s) layer structures were found which lead to an anisotropy in the  $xy$  plane.<sup>15</sup> But even for a 9.7% duplex  $a$  deformed sample ( $v = 8 \times 10^{-4}$  mm/s) a homogeneous distribution of etch pits of the order  $10^8$  cm<sup>-2</sup> could be obtained.<sup>5</sup>

#### IV. EXPERIMENTAL

Our samples were cut from Czochralski-grown single crystals with an acid string saw in order to avoid unnecessary lattice damage. The specimens were etched with great care to a thickness between 0.5 and 1 mm. This is sufficiently thin to guarantee a homogeneous damage rate in the bulk material if the samples are bombarded with 20-MeV electrons because the penetration depth for electrons with this energy is about 1 cm in Te. The irradiations were

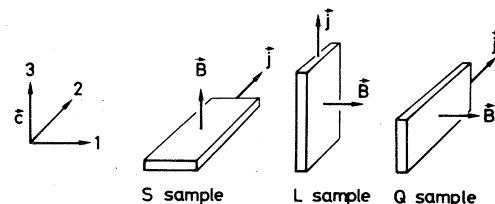


FIG. 2. Sample orientations in the crystal.

performed with a 35-MeV Betatron with an external beam guide system at temperatures of 10 and 35 K. The direction of the electron beam was parallel to the magnetic field. To avoid surface effects the specimens were rinsed with ammonia (Sec. II). The rod-shaped *S* and *L* samples (Fig. 2) were provided with five contacts in the usual way. In the case of the quadratic *LQ* sample (combination of *L* and *Q* samples) eight probes were necessary to measure the galvanomagnetic properties parallel and perpendicular to the *c* axis in the same sample. The measurements of  $\rho$  and  $R_H$  were performed under constant current conditions with conventional dc techniques; the influence of the sample geometry was considered according to the technique of Vogler.<sup>18</sup> The scattering factor was determined to be 1.0 at 35 K for the used magnetic field of about 0.1 T for *S* as well as *L* samples. This result was drawn from measurements of the Nernst-Ettingshausen coefficient of samples irradiated with 1-MeV electrons.<sup>19</sup> Therefore the interpretation  $p = 1/eR_H$  and  $\mu_{\text{Drift}} = \mu_{\text{Hall}}$  is justified.

In Table I the typical parameters of the investigated samples (orientation, degree of deformation  $\Delta l/l$ , initial hole concentration  $p_\infty$ , and maximal irradiation dose  $\phi_{\text{max}}$ ) are summarized. Samples 3 and 4 were cut from crystals doped with antimony with an average Sb concentration of  $1 \times 10^{14}$  at. Sb  $\text{cm}^{-3}$  and  $5 \times 10^{14}$  at. Sb  $\text{cm}^{-3}$ , respectively. The sample notation 4/1 and 4/2 indicates, e.g., that the specimens were prepared from adjacent regions of a particular single crystal and should have the same carrier concentration. If there are differences, they can be attributed largely to the experimental error in the determination of the Hall coefficient, caused mainly by uncertainties in the geometry of the specimens. Samples 5 and 6 are deformed under duplex *a* conditions at room temperature.

## V. IRRADIATION-INDUCED ACCEPTOR LEVELS

The elemental semiconductor Te is always *p* type in the extrinsic range. The positions of the acceptor levels can be determined under certain conditions from the temperature dependence of the Hall coefficient. If we assume *n* acceptor levels  $E_{A_i}$  the hole density of the unirradiated sample is given by

$$p = \sum_{i=1}^n N_{A_i}^- = \sum_{i=1}^n N_{A_i} \left[ 1 + g_{A_i} \exp \left( \frac{E_{A_i} - E_F}{k_B T} \right) \right]^{-1} \quad (4)$$

$N_{A_i}$  is the concentration of acceptors with energy  $E_{A_i}$  and  $g_{A_i}$  is the degeneracy factor.<sup>20</sup> Knowing the hole density  $p$  and the temperature  $T$ , we can calculate the associated Fermi energy  $E_F(p, T)$  from

$$p = \int_{-\infty}^{E_{\text{max}}} D(E) f_p(E, E_F, T) dE \quad (5)$$

where  $f_p(E, E_F, T)$  is the Fermi distribution for holes. The density of states  $D(E)$  is determined from a valence-band model as proposed by Bangert *et al.*<sup>21</sup> Using (4) and (5) we make a fit of the temperature dependence of the hole concentration. In the case of the stronger doped sample 4/2 we can neglect those levels which are not caused by the impurity atoms. Figure 3 shows that we can fit to the  $p(T)$  curve satisfactorily with only one fit parameter  $E_{A_1}$ . The fit is quite good for an acceptor energy of  $E_{A_1} \approx 1$  meV. This is in agreement with the values found by other methods. Impurity atoms such as antimony are associated with an energy level between 1 and 1.5 meV.<sup>22</sup> (The zero point coincides with the valence-band edge.)

TABLE I. Typical parameters for the samples investigated.

Sample	1	2	3/1	3/2	4/1	4/2	5/1	5/2	6	7	8/1	8/2
Orientation	<i>S</i>	<i>S</i>	<i>S</i>	<i>S</i>	<i>S</i>	<i>S</i>	<i>S</i>	<i>S</i>	<i>S</i>	<i>L</i>	<i>LQ</i>	<i>LQ</i>
$p_\infty$ (10 K) ( $10^{13} \text{ cm}^{-3}$ )	3	4	14	12	78	71	4	5	23	3	3	3
$\phi_{\text{max}}$ ( $10^{12} \text{ cm}^{-2}$ )	11	88	8	88	35	87	12	87	86	7	3	140
Deformation (%)	0	0	0	0	0	0	1.9	1.9	3.7	0	0	0

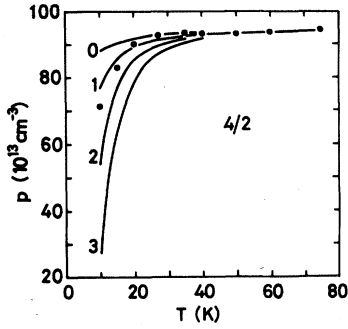


FIG. 3. Temperature dependence of the hole concentration for a stronger doped sample (sample 4/2). ●, measured; —, calculated (the numbers next to the curves stand for the fit parameter  $E_{A_1}$  in meV).

Our irradiation experiments at low temperatures with 20-MeV electrons showed that the hole concentration  $p$  increases linearly with the irradiation dose  $\phi$ ,<sup>23,24</sup> except for sample 2, which showed a slight downward curvature (Fig. 4) and the deformed specimen 6 for which the data are shown in Fig. 16. The same behavior was found after 1-MeV irradiation.<sup>25</sup> The increase of the hole concentration due to the generation of point defects by electron irradiation causes a decrease of the Fermi energy  $E_F$ . From this, we can find out in principle where the

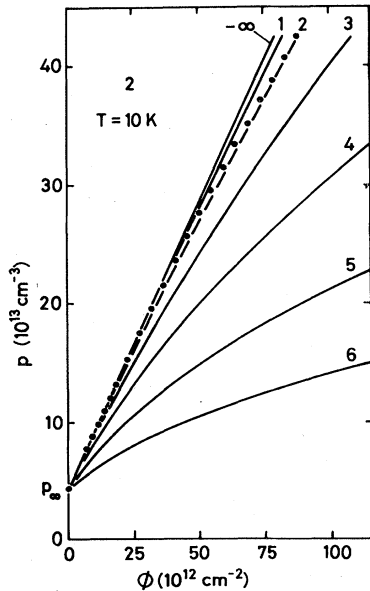


FIG. 4. Dose dependence of the hole concentration for an undoped undeformed S sample (sample 2) by 20-MeV electron irradiation at 10 K. ○, measured; —, calculated (the numbers next to the curves stand for the fit parameter  $E$  in meV).

radiation-induced levels are located, and we can also investigate the influence of those acceptor levels which are already present in the unirradiated samples.

The comparison of the 1- and 20-MeV data shows that the irradiations produce mainly vacancies and interstitials. According to semiempirical calculations for Te model crystals by Weigel *et al.*,<sup>26</sup> vacancies generate shallow acceptor levels, whereas the interstitials can act as deep donors only. Therefore we proceed from the assumption that vacancies act as acceptors, and firstly we suppose that the interstitials act as donors. Moreover, we assume that the irradiation produces the same concentration of vacancies and interstitials and that their number increases proportionally with the irradiation dose, which means  $N_A = N_D = c\phi$ ,  $c = \text{const}$ , where  $N_A$  is the concentration of acceptors with energy  $E_A$  and  $N_D$  the concentration of donors with energy  $E_D$  created by irradiation. Then we get for the hole concentration as a function of the irradiation dose

$$p(\phi) = N_A^-(\phi) - N_D^+(\phi) + \sum_{i=1}^n N_{A_i}^-(\phi) \quad (6)$$

$\sum_{i=1}^n N_{A_i}^-(\phi)$  are the holes produced by those levels which are already present in the unirradiated samples,

$$N_A^-(\phi) = N_A \{ 1 + g_A \exp[(E_A - E_F)/k_B T] \}^{-1} \quad (7)$$

are the holes produced by the irradiation-induced acceptor levels, and

$$N_D^+(\phi) = N_D \left[ 1 + \frac{1}{g_D} \exp[(E_F - E_D)/k_B T] \right]^{-1} \quad (8)$$

are the holes which are trapped by the irradiation-induced donor levels.

For special cases, we can neglect the depopulation of those levels which are present in the unirradiated sample, which means that we can substitute  $\sum_{i=1}^n N_{A_i}^-$  by the initial concentration  $p_\infty$ . With  $\Delta p(\phi) = p(\phi) - p_\infty$  and  $N_A = N_D = c\phi$ ,  $c = \text{const}$ , we get from (6), (7), and (8):

$$\Delta p(\phi) = \left[ \frac{1}{1 + g_A \exp[(E_A - E_F)/k_B T]} - \frac{1}{1 + \frac{1}{g_D} \exp[(E_F - E_D)/k_B T]} \right] c\phi \quad (19)$$

If  $E_A \ll E_F$  and  $E_D \ll E_F$ , then the hole density

increases proportionally with the irradiation dose:  $\Delta p(\phi) = c\phi$ . If the irradiation-induced acceptor and donor levels are depopulated, then the measured  $p(\phi)$  curves should have a clockwise curvature (Fig. 4). We cannot distinguish whether only the acceptors or donors or both of them are involved in this depopulation. Therefore we can only determine the maximal possible values of either  $E_A$  or  $E_D$ , by setting  $E_D = -\infty$  or  $E_A = -\infty$ . The factors  $g_A$  and  $g_D$ , which can only be  $\frac{1}{2}$  or 2,<sup>20</sup> are chosen for this estimation such that  $E_A$  and  $E_D$ , respectively, are maximal, i.e.,  $g_A = g_D = \frac{1}{2}$ .

For

$$\frac{1}{1 + \frac{1}{2} \exp[(E - E_F)/k_B T]} = 1 - \frac{1}{1 + 2 \exp[(E_F - E)/k_B T]}$$

we can try to fit to the measured curves—considering (5)—by

$$\Delta p(\phi) = \frac{c\phi}{1 + \frac{1}{2} \exp[(E - E_F)/k_B T]}, \quad (10)$$

with the fit parameters  $c$  and  $E$ , where  $E$  stands for  $(E_A)_{\max}$  and  $(E_D)_{\max}$ , respectively. In this way, we find  $E_A < 2$  meV,  $E_D < 2$  meV for the 20-MeV experiments. This result is illustrated in Fig. 4 for the undoped and undeformed Te sample 2 with an initial hole concentration of about  $4 \times 10^{13} \text{ cm}^{-3}$  at 10 K. The measured hole concentration  $p$  as a function of the irradiation dose  $\phi$  is represented by the circles. The solid curves represent calculated values, and the numbers next to the curves stand for the fit parameter  $E$  in meV.  $c$  is fixed by the initial slope of the measured curve.

The Fermi level could be lowered further by the previous 1-MeV irradiations because at this energy the Van de Graaff generator used could reach doses that were orders of magnitude higher. If we apply our method to the 1-MeV measurements,<sup>4</sup> we find  $E_A < 0$  meV,  $E_D < 0$  meV. On the other hand, Safert *et al.*<sup>4</sup> computed from the  $p(\phi)$  curves of the 1-MeV experiments that  $E_A = 15 \pm 5$  meV and  $0 < E_D < 50$  meV. They obtained this different result because in their analysis they made the invalid assumption  $E_F \ll E_D$ . Our result is in agreement with that of Koma and Tanaka,<sup>27</sup> who concluded from their measurements that the acceptor levels of the lattice defects produced by 1.5-MeV electron irradiation are located in the valence band as considered by Takita *et al.*<sup>28</sup> Most of the 20- and 1-MeV irradiation experiments yielded a linear depen-

dence of the generated excess hole concentration on the electron dose. This results in negative acceptor and donor binding energies, which means that both energy levels are located inside the valence band.

We chose the data of sample 2 for the evaluation of an upper limit for  $E_A$  and  $E_C$ . Because electrons have never shown up in low-temperature transport measurements on tellurium, one must conclude that the donor level is located below the acceptor and that no self-compensation occurs. An estimate of the concentration of Frenkel defects from the cross section of 20-MeV electrons which tellurium atoms and the multiplication factor shows that it is reasonable to conclude that each vacancy-interstitial pair generates one hole, but no electron.

## VI. MOBILITY INCREASE DUE TO ELECTRON IRRADIATION

Contrary to other materials, the creation of lattice defects in Te by low-temperature irradiation with high-energy electrons can lead to an increase of the hole mobility. 1-MeV irradiations at 35 K produce a maximal rise of less than 40% for samples with  $\vec{j} \perp c$ , whereas for  $\vec{j} \parallel c$  the mobility is lowered from the beginning of the irradiation. This behavior was quantitatively described<sup>4</sup> by a model based on the assumption that the dislocations act as saturable traps for the vacancies and that this process lowers the scattering efficiency of the dislocations in the case of  $\vec{j} \perp c$ .<sup>3</sup> For  $\vec{j} \parallel c$  it was additionally assumed that in a particular volume around the dislocations, no carrier transport takes place so that the mobility should only decrease due to the radiation defects remaining in the bulk material. Contrary to the last assumption we also found for  $\vec{j} \parallel c$  a rise of maximal 250% (Fig. 5). Moreover, the relative mobility

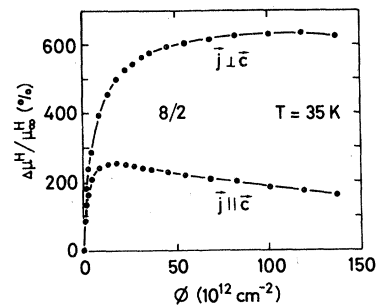


FIG. 5. Dose dependence of the relative change in Hall mobility for the two orientations of an undoped and undeformed LQ sample (sample 8/2) by 20-MeV electron irradiation at 35 K.

change  $(\mu^H - \mu_\infty^H)/\mu_\infty^H$ ,  $\mu_\infty^H$  being the preirradiation value of  $\mu^H$ , is strongly dependent on the doping, which is not involved in the model presented above. Figure 6 shows this behavior for differently doped *S* samples ( $j \perp c$ ) at an irradiation temperature of 10 K. For undoped samples (1 and 2) we reached increases of up to 700%, whereas the slightly doped specimen 3/2 shows only a maximal rise of about 10%. A somewhat stronger doping (cf. sample 4/2) causes a mobility decrease from the outset of the irradiation. (3/2 and 4/2 are associated with the strongly stretched scale on the right-hand side.)

We can understand this doping dependence by looking at the mobility as a function of the hole concentration in Fig. 7. In this figure, the mobility values of differently doped *S* samples are plotted for three temperatures; the solid symbols stand for unirradiated samples, while the open symbols designate the same, but irradiated samples. For the mobility dependence on the carrier concentration it does not seem to matter whether the carrier increase is due to doping or irradiation. If one wants to maintain the explanation of the strong mobility increase of the undoped samples in the case of the irradiations as being due to the vacancy-dislocation mechanism, then one is tempted to assume that the initial mobility of the slightly doped samples, which is several times higher than that of the undoped samples, is caused by an analog of the impurity-atom-dislocation mechanism. However, it is more probable that in both cases the essential shielding of the dislocations is due to the free carriers. This assumption is also supported by the fact that we could reach mobility increases of 100% at 10-K irradiations for pure samples with such small doses that only 1 vacancy per 1000 atomic chains per mm

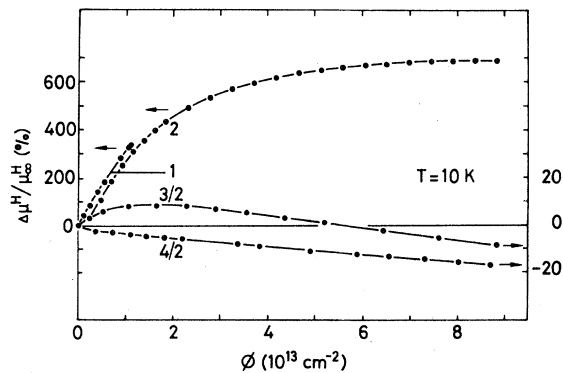


FIG. 6. Dose dependence of the relative change in Hall mobility for differently doped undeformed *S* samples (see Table I) by 20-MeV electron irradiation at 10 K (Ref. 31).

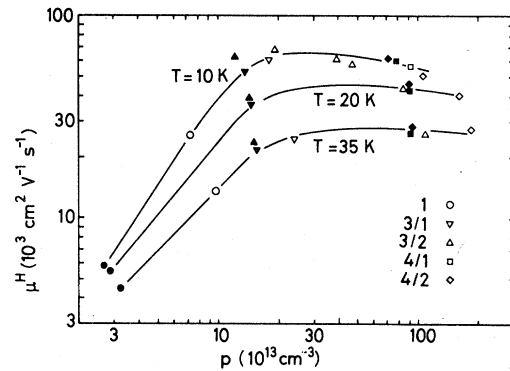


FIG. 7. Hall mobility of differently doped unirradiated (solid symbols) and irradiated (open symbols) undeformed *S* samples (see Table I) as a function of the hole concentration at various temperatures (Ref. 31).

thickness was created. Considering that the vacancies are not mobile at this temperature, and that their shielding of the dislocations, if it exists at all, requires relatively small distances and that therefore the dislocations would have to attract the vacancies over extremely long distances to gather a sufficient number around them, the whole process does not seem plausible. The shielding of the dislocations by the free carriers can be imagined as follows: The dislocations are surrounded by a region of enhanced hole concentration (dislocation screening region), whereas the rest of the crystal (bulk material) is depleted of holes. If the total hole density is increased by irradiation or doping, then a saturation of the dislocation screening regions with holes will take place and the concentration of holes in the bulk material will increase. This will cause an increase of the measured effective mobility if the mobility in the bulk material is higher than that in the dislocation screening region. Because the mobility in the bulk decreases with increasing defect concentration, the measured mobility will pass through a maximum. Abokarov *et al.*<sup>9</sup> conclude from quenching experiments that the holes which are already present in undoped undeformed samples (with a hole density of a few times  $10^{13} \text{ cm}^{-3}$ ) are dislocation induced. They assume that the dislocations capture electrons, whereby they become negatively charged. The holes created in this way form screening cylindrical regions with high hole densities around the dislocations. If the dislocations are completely screened in a crystal with no current, then this screening is preserved if the current is parallel to the dislocations (*L* samples). If the current is perpendicular to the dislocations (*S* and *Q* samples), the holes are forced to leave the screening regions.

Therefore, for additional holes produced by irradiation, quenching, or doping, the dislocations are not completely screened. As a consequence the maximum of the mobility is reached for  $\vec{j} \perp c$  at an essentially higher hole concentration than for  $\vec{j} \parallel c$  (Fig. 8) if we create additional holes by electron irradiation. Consequently, we can start from the following simple assumptions in the case of the  $L$  orientation:

- (1) In the unirradiated crystal all present holes ( $p_{\text{disl}}$ ) move in the dislocation shielding region with the mobility  $\mu_{\text{disl}}$ .
- (2) The irradiation-induced holes are not required for screening and can therefore move in the bulk material. Their density is  $p - p_{\text{disl}}$ , where  $p = 1/eR_H$  is the total hole density.
- (3) The mobility of the holes is smaller in the dislocation screening region than in the material which is free of dislocations:

$$\mu_{\text{disl}} < \mu_{\text{bulk}} .$$

Hence for the conductivity

$$\sigma = ep_{\text{disl}}\mu_{\text{disl}} + e(p - p_{\text{disl}})\mu_{\text{bulk}}$$

with which we get for the effective mobility

$$\mu^H = \sigma R_H = [p_{\text{disl}}\mu_{\text{disl}} + (p - p_{\text{disl}})\mu_{\text{bulk}}]/p .$$

So we can explain the curvature of the experimentally found mobility  $\mu^H$  as a function of the total hole density  $p$  (Fig. 8) in the following way: At first ( $p = p_{\text{disl}}$ ) we measure the hole mobility in the screening region ( $\mu^H = \mu_{\text{disl}}$ ), then a composite quantity, and finally for  $p \gg p_{\text{disl}}$  the mobility in the dislocation-free crystal ( $\mu^H \approx \mu_{\text{bulk}}$ ). According to this model we can compute the mobility in the dislocation-free region from measured values as follows:

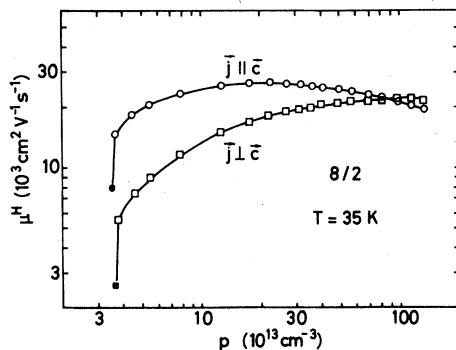


FIG. 8. Hall mobility for the two orientations of an undoped undeformed  $LQ$  sample (sample 8/2) as a function of the hole concentration by 20-MeV electron irradiation at 35 K.

$$\mu_{\text{bulk}} = (p\mu^H - p_{\text{disl}}\mu_{\text{disl}})/(p - p_{\text{disl}}) .$$

Looking at Fig. 9 we notice that  $1/\mu_{\text{bulk}}$  increases proportionally to the defect concentration as predicted by theory.<sup>20</sup> Moreover, we can see from the measured quantity  $1/\sigma R_H$  that for  $\vec{j} \parallel c$  already a small carrier increase is insufficient to outweigh the influence of the dislocations.

For  $p \gg p_{\text{disl}}$  that means in the range where  $\mu^H \approx \mu_{\text{bulk}}$  it can be seen from Fig. 8 that the anisotropy of the Te lattice causes no significant influence on the mobility. This is in agreement with measurements on doped samples ( $p \approx 3 \times 10^{15} \text{ cm}^{-3}$ ) where no anisotropy of the galvanomagnetic properties could be found.<sup>29</sup> On the other hand, there is a strong anisotropy of the mobility ( $\mu_{\infty}^{\parallel} \approx 5\mu_{\infty}^{\perp}$  at 10 K in the unirradiated sample caused by the dislocations oriented parallel to the  $c$  axis. (The hole densities appertaining to Fig. 8 differ at most by 3% at the same dose.)

The undeformed samples used in the 1-MeV experiments had a hole density of about  $5 \times 10^{14} \text{ cm}^{-3}$ . Figure 8 shows that for this concentration the mobility has already passed its maximum for  $\vec{j} \parallel c$ . Therefore only a mobility decrease due to electron irradiation was found for  $L$  samples. On the other hand, the maximum is almost reached in the case of  $\vec{j} \perp c$ . Thus a small mobility enhancement for  $S$  samples could still be obtained.

Now we can also explain the extreme mobility increases of more than 3000% obtained in 1-MeV experiments with duplex  $a$  deformed  $S$  samples by Roos.<sup>5,25</sup> These samples were cut, like our undoped samples, from purer crystals with an initial hole concentration of some  $10^{13} \text{ cm}^{-3}$  due to advances

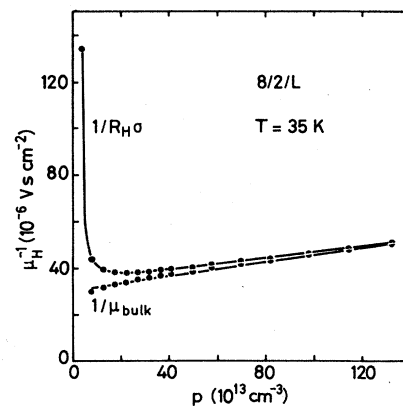


FIG. 9. Reciprocal mobility of the dislocation-free region  $1/\mu_{\text{bulk}}$  calculated from the measured Hall mobility  $\sigma R_H$  for an undoped and undeformed  $L$  sample (sample 8/2  $L$ ) by 20-MeV electron irradiation at 35 K.



in the crystal preparation. According to our model the mobility should decrease with increasing dislocation density for samples with  $\vec{j} \perp c$ . Consequently, the maximal rise of the relative mobility change should increase with increasing degree of deformation. Moreover, a higher hole density is required for a higher dislocation density to reach the maximum of the mobility. This was experimentally found.<sup>5</sup>

On the other hand, in the case of  $\vec{j} \parallel c$  the increase of the dislocation density should not alter the mobility. This was found by Abakarov *et al.*<sup>14</sup> for annealed samples (cf. Sec. VIII). Immediately after deformation they obtained an increase of the mobility for  $\vec{j} \parallel c$ . According to our model this can be explained by the fact that during the deformation, point defects were also produced in the bulk material, which causes an enhancement of the hole density in the dislocation-free region.

The suggested model has, for the time being, only qualitative character. It is obvious that a two-carrier model should be used for the analysis of the Hall data. In principle, one could obtain information about the ratio of holes in the regions around the dislocations and in the bulk and the respective mobilities from the magnetic field dependence of the Hall constant. This, however, would require magnetic fields of the order 10 T, which unfortunately were not available in the cryostat used; the data were taken in fields of less than 0.1 T.

It seems that the line character of the dislocations does not influence the magnitude of the low-field Hall coefficient significantly, because within the experimental accuracy  $R_H$  is the same for the two magnetic field orientations parallel and perpendicular to the  $c$  axis. An estimate of the size of the space-charge cylinder around the dislocations is rather difficult because of the high concentration of electrons on the dislocations, which should give rise to many-body effects. We intend, however, to look into these problems in some detail in the future.

So far, no non-Ohmic effects have been found in very pure tellurium samples at helium temperatures in zero magnetic field at electric fields of the order 1 V/cm. No strong deviations from linear current-voltage characteristics are expected anyway, because with a binding energy of 3 meV of dislocation bound holes, most of the carriers are no longer located at 35 K, the temperature at which the data shown in Fig. 8 were taken. Owing to the relatively weak binding energy, deviations from Ohm's law might occur already at rather small electric fields, and it seems possible that the nonlinearities escaped detection.

## VII. ISOCHRONALS

It was shown<sup>30</sup> that isochronal annealing experiments are especially appropriate to investigate the recovery behavior of electron-irradiated Te. Therefore we determined the hole density  $p$  and the mobility  $\mu^H$  at a reference temperature  $T_R = 35$  and 20 K, respectively, after an annealing of 10-min duration at successively higher annealing temperatures  $T_A$  up to 315 K. The heating and cooling times increased with the annealing temperatures; however, in the ranges in which quantitative analyses were performed, they were short compared with the annealing time, especially in the range of the first recovery stage (several seconds). Typical isochronal annealing curves—for differently doped undeformed  $S$  samples (see Table I)—are plotted in Fig. 10, showing the unannealed fraction

$$\varphi_p(T_A) = (p - p_\infty)/(p_0 - p_\infty) ,$$

where  $p_\infty$  is the preirradiation and  $p_0$  the postirradiation value of the hole concentration  $p$ . The following remarkable properties can be seen:

- (1) An especially sharp pronounced recovery stage at 50 K (first stage).
- (2) The number of holes increases again after the first stage up to about 90 K.
- (3) A recovery stage between 100 and 150 K (second stage).
- (4) A recovery stage above 200 K (third stage).

The isochronal annealing studies were performed for all samples summarized in Table I. Figure 11 shows the carrier isochronals for undoped  $S$  samples with different degree of deformation. We determined the activation energy  $E_a$  and the order of reaction  $\gamma$  for stage 1 for each carrier isochronal. We obtained the following result, independent of the dose, the doping, the deformation, and the orientation<sup>31</sup>:

$$E_a = 170 \pm 30 \text{ meV}, \quad \gamma = 1 \pm 0.1 .$$

Moreover,

- (1) The first stage always lies at  $T_A = 49 \pm 1$  K.
- (2) The same percentage of carriers always vanishes in the first stage for the investigated  $S$  samples (13%, see Fig. 12).

This indicates a vacancy-interstitial annihilation with its own partner. This agrees also with the fact that in the first stage of the 1-MeV measurements (which was detected exactly at the same temperature) a clearly higher percentage of holes (about 35%) vanished (Fig. 13). If the energy of the irradiation particles is only a little higher than the thresh-

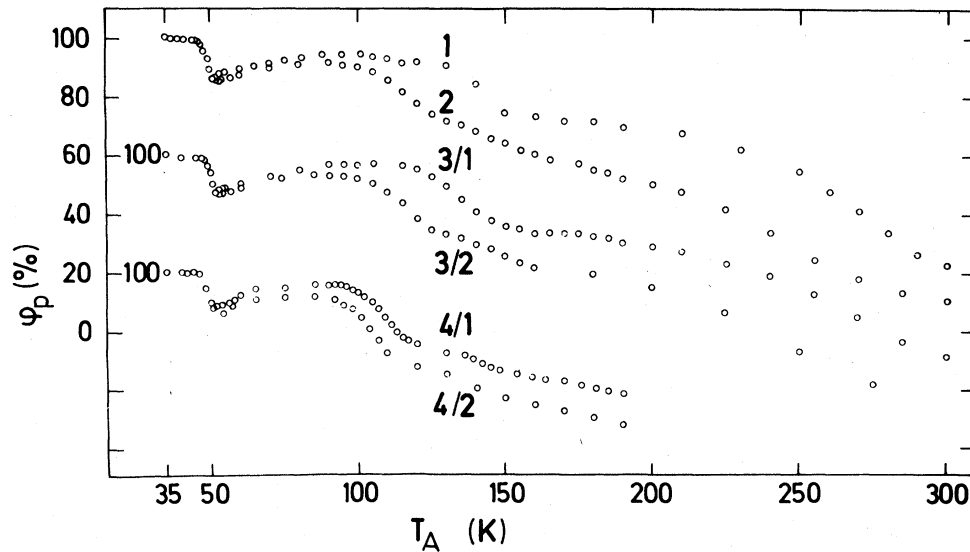


FIG. 10. Unannealed fraction of the hole concentration for differently doped undeformed *S* samples irradiated with different electron dose (see Table I) as a function of the annealing temperature (Ref. 31).

old energy, mostly vacancy-interstitial pairs with small distances between the partners should be created.

These conclusions differ from those drawn due to the 1-MeV experiments, where it was assumed that a "defect rearrangement" occurs in stage 1 whose microscopic nature was not yet known.<sup>4</sup> The basis of that consideration was the experimental result that, independent of the irradiation dose, the same number of defects should always recombine. The data shown in Fig. 12, which have a considerably

higher precision than the 1-MeV results (Fig. 13), indicate, however, that the same percentage of defects always recombines. Inspection of the original 1-MeV data shows that a reinterpretation is possible if the experimental scatter is taken into account (Fig. 13) and if the data point for the highest dose (full symbol in Fig. 13) is omitted. Scrutiny of the original recordings for the highest dose reveals obscure discontinuities in the Hall voltage during the irradiation as well as during the annealing, which allows us to ignore these data.

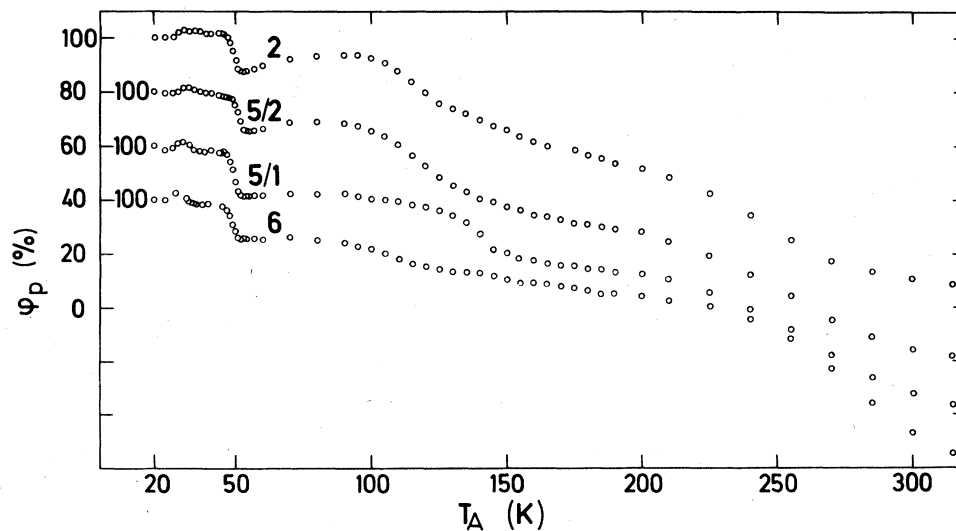


FIG. 11. Unannealed fraction of the hole concentration for undoped *S* samples with different degrees of deformation irradiated with different electron doses (see Table I) as a function of the annealing temperature.

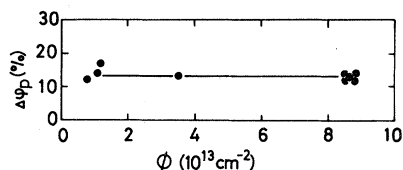


FIG. 12. Fraction of the hole concentration annealed in the 50-K stage as a function of the irradiation dose for all *S* samples (see Table I) of the 20-MeV investigations.

Now we can also understand the behavior of the mobility isochronals in the first stage. Looking at the isochronals of the Hall mobility  $(\mu^H - \mu_\infty^H)/\mu_\infty^H$  in Figs. 14 and 15, we can perceive a decrease (samples 1, 3/1), no changes (sample 2), or an increase (sample 3/2) in stage 1 dependent on the dose. Moreover, a strong dependence on the doping is displayed by the mobility isochronals as opposed to the carrier isochronals. The influence of doping and dose on the formation of the 50-K stage becomes clear with the consideration of the dependence of the mobility on the carrier concentration in Fig. 7. This  $\mu(p)$  relation comes about as follows. Firstly, the irradiation defects as well as the impurity atoms act as scattering centers. Secondly, they produce dislocation-shielding free carriers. The recombination of close pairs means that the  $\mu(p)$  relation is passed through backwards from larger to smaller  $p$  values. So a decrease of the carrier concentration causes a mobility decrease in the range before the maximum of the mobility and an increase in the

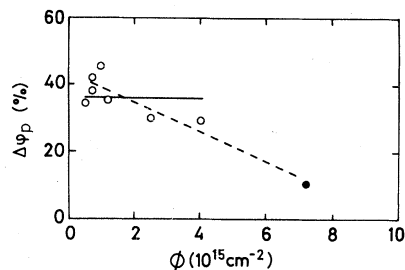


FIG. 13. Fraction of the hole concentration annealed in the 50-K stage as a function of the irradiation dose for the undoped undeformed *S* samples of the 1-MeV measurements (Ref. 2).

range after the maximum. There is no change in the plateau region.

To prove this assumption, we calculate mobility isochronals from the carrier isochronals and from the  $\mu(p)$  curves which were obtained during the irradiation. Then we compare these calculated values with the measured isochronals. As can be seen in Figs. 14 and 15, the calculated and the measured curves agree in the region of stage 1. This holds for all investigated samples independent of doping, dose, orientation, and deformation.

All data indicate that in stage 2 an uncorrelated vacancy-interstitial recombination takes place. For example, the onset of stage 2 shifts from about 150 K to about 100 K with increasing dose (Figs. 10 and 11). The analysis of the carrier isochronals

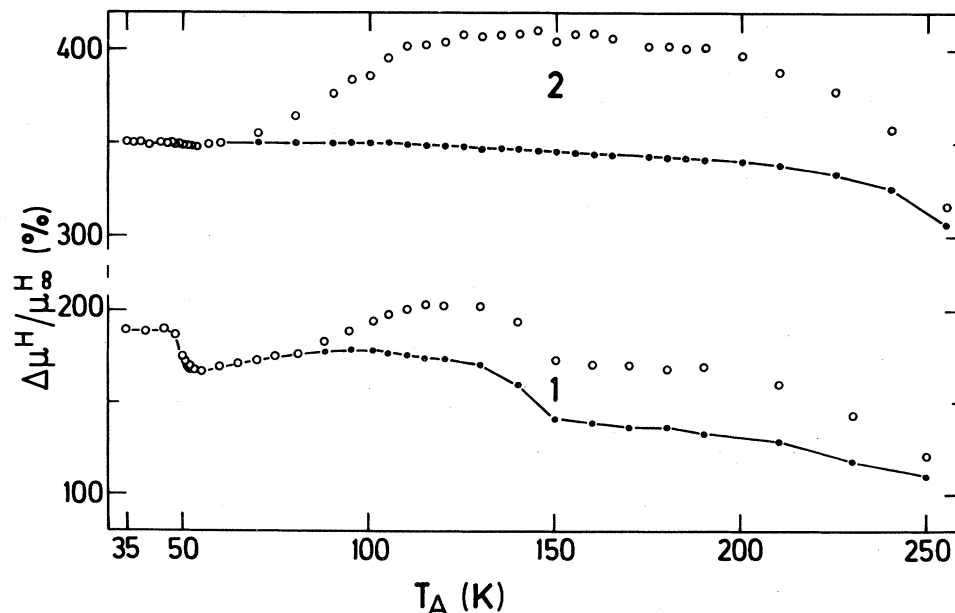


FIG. 14. Annealing curves of the relative change in Hall mobility for undoped undeformed *S* samples for different electron doses (see Table I).  $\circ$ , measured;  $\bullet$ , calculated. (Ref. 31).

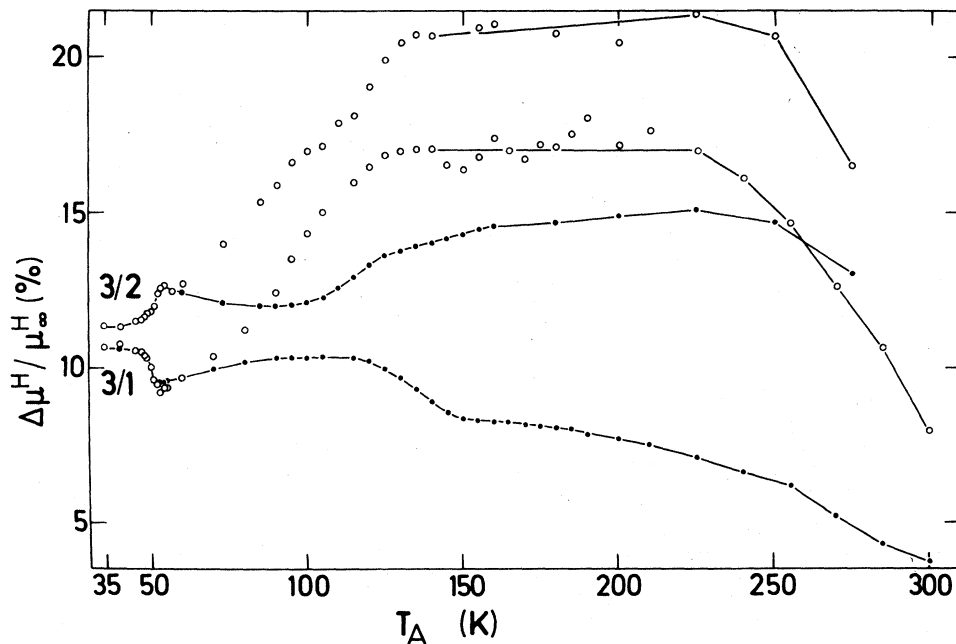


FIG. 15. Annealing curves of the relative change in Hall mobility for slightly doped undeformed *S* samples for different electron doses (see Table I).  $\circ$ , measured;  $\bullet$ — $\bullet$  calculated. (Ref. 31).

shows, however, that the order of the reaction is between 1 and 2. This behavior can be explained by the fact that the dislocations capture a fraction of the mobile defects before the defects find a recombination partner. This view is supported by the fact that the percentage of the carriers vanishing in stage 2 decreases with increasing dislocation density (Fig. 11). Such a capture also explains the additional increase of the measured mobility isochronals after stage 1 (Figs. 14 and 15). The migration of neutral interstitials into the dislocation screening region would enhance the bulk mobility, because scattering centers vanish from the bulk material. As the distribution of the holes in the crystal is not changed by this process, an increase of the measured mobility will occur. This additional rise cannot be seen in the calculated curves (Figs. 14 and 15), because such a change of the  $\mu(p)$  relation is not considered. If, instead of the interstitials, the negatively charged vacancies are captured, the situation is still more complicated, because the distribution of the holes in the crystal is also altered. In this case the dislocations can act only as traps, not as sinks, because no carriers vanish at these annealing temperatures. Since we cannot distinguish from our experiments whether the vacancies or the interstitials interact with the dislocations, there are alternative possibilities for the annealing process in the third stage, where all irradiation-induced defects vanish.

Contrary to the additional mobility increase after the 50-K stage which was also found in the 1-MeV experiments, the small rise of the hole density after stage 1 should be a minor effect. Since this increase could not be seen in the 1-MeV carrier isochronals, it could be caused by the higher irradiation energy. Also, the dislocations should be involved in this process, because the rise of the carrier isochronals after stage 1 decreases with increasing degree of deformation (Fig. 11).

A pronounced recovery stage at 35 K was found for the pure, deformed *S* samples of the 1-MeV measurements.<sup>5</sup> Our carrier isochronals (Fig. 11) verify the existence of a 35-K stage. However, the effect is very small and the available data are scarce, so it seems premature to make any statements about the nature of this stage.

In addition, small stages at 140 and 180 K occurred in the 1-MeV experiments with undeformed samples ( $p \approx 5 \times 10^{14} \text{ cm}^{-3}$ ),<sup>2,3</sup> but they could not be found in the carrier isochronals of the deformed samples<sup>5,25</sup> which were cut from purer crystals with a hole density of some  $10^{13} \text{ cm}^{-3}$ . In the case of the 20-MeV experiments, there was no 180-K stage, whereas the 140-K stage seemed to exist for the more strongly doped sample 4/1 ( $p \approx 7 \times 10^{14} \text{ cm}^{-3}$ ). This could be an indication that an interaction between irradiation-induced defects and impurity atoms also takes place.

### VIII. DEFORMATION-INDUCED ACCEPTOR LEVELS

Doukhan *et al.*<sup>12</sup> conclude from their measurements that the hole concentration is not altered by the generation of *a* edge dislocations due to a *a* deformation, because these dislocations do not break the strong bonds within the chains (Sec. III). However, it must be considered that the mean value of the hole densities for the samples investigated by these workers was about  $6 \times 10^{14} \text{ cm}^{-3}$  and that the variations between the Hall coefficient of deformed and undeformed samples of the same orientation which were declared as "not remarkable" total up to 50%. Therefore we assume that a dislocation-induced enhancement of the hole concentration of a few  $10^{14} \text{ cm}^{-3}$  (cf. samples 2 and 6 in Table I) was not detectable within the limits of the experimental accuracy of Doukhan *et al.* Moreover, von Alpen *et al.*<sup>10,11</sup> found in optical measurements of identically deformed samples dislocation-induced levels located 3 meV above the valence-band edge. Although they estimate jog densities of about  $10^{14} - 10^{15} \text{ cm}^{-3}$  for 4% deformed samples during duplex *a* deformation, they conclude from their experiments that the bound states are not due to the broken covalent bonds caused by jogs.

Furthermore, in all other attempts, the *a* deformation leads to an increase of the hole density<sup>13,14</sup>; the investigators at the University of Würzburg always find an enhancement for duplex, as well as for simplex *a* deformed samples (see, e.g., Ref. 5). During plastic deformation not only does the dislocation density increase, but also point defects are created. Therefore we annealed the deformed samples at room temperature before taking data. Since we know from our experiments that the recovery of the electrical properties of electron-irradiated Te is complete at room temperature, those charge carriers which are due to deformation and do not vanish by room-temperature annealing should be dislocation induced. We find a charge density per dislocation of one-half an elementary charge per angstrom. (This value may be an order of magnitude smaller because of the uncertainty in the determination of the dislocation density.) Nearly the same value ( $0.8e/\text{\AA}$ ) was obtained by Abokarov *et al.*<sup>9</sup> in experiments with inhomogeneously deformed samples.

Several reasons are conceivable for the existence of acceptor states attributed to dislocations which were created by *a* deformation. Faivre<sup>13</sup> asserts that the majority of the dislocations does not consist of pure *a* edge dislocations, but is of a mixed charac-

ter. If only *a* edge dislocations are generated, jogs may, after all, be important. However, even in the case of no broken covalent bonds, bound states should occur due to the lattice deformation caused by the dislocations.<sup>32-34</sup>

Figure 16 shows the dose dependence of the hole density for the undoped 3.7% deformed sample 6 irradiated at 10 K (upper curve). If we assume that in the unirradiated sample all holes ( $p_\infty$ ) are produced by 3-meV levels, then we can calculate—considering Eq. (5)—the depopulation of these 3-meV levels with increasing dose (lower solid curve in Fig. 16). This emptying causes a decreasing anticlockwise curvature of the measured curve (upper curve) with increasing dose. If we subtract the lower from the upper curve, we obtain the concentration of the irradiation-induced holes, which increases at first proportionally with the irradiation dose as expected. The deviation from a straight line at the highest doses can be explained again by the depopulation of the irradiation-induced levels. (We do not consider higher levels at 8, 15, and 20 meV which were also attributed to deformed samples due to measurements of the far-infrared photoconductivity,<sup>35</sup> because they would be depopulated at 10 K.)

The interpretation of the  $\mu(p)$  curve for the undoped undeformed *L* sample (Fig. 9) by the proposed model is a hint that also the "natural" dislocations in Te are negatively charged. In addition to the above-mentioned mechanisms, an attachment of point defects to the dislocation core is also possible.

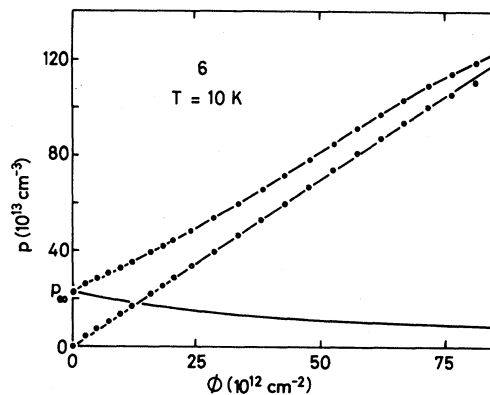


FIG. 16. Dose dependence of the hole concentration for an undoped 3.7% deformed *S* sample (sample 6) by 20-MeV irradiation at 10 K (upper curve). The lower solid curve shows the calculated depopulation of the levels which are already present in the unirradiated sample, if it is assumed that in this case all holes are produced by 3-meV levels. If we subtract the lower from the upper curve we obtain the concentration of the irradiation-induced holes (curve starting at the origin).

We require more detailed information about the microscopic properties of the dislocations in Te to answer these questions completely. This will be a task for the future.

### IX. CONCLUSION

A systematic variation of the concentration of impurity atoms, Frenkel defects, and dislocations by doping, irradiation, and deformation, yielded interesting information about the influence of lattice defects on the transport properties of the elemental semiconductor tellurium. Our data—as well as the results of quenching and irradiation experiments of other investigators—can be interpreted as follows.

(1) The strong anisotropy of the low-temperature mobility of undoped Te samples with a hole concentration of a few  $10^{13} \text{ cm}^{-3}$  is caused by the dislocations oriented parallel to the crystallographic  $c$  axis.

(2) The dislocations are surrounded by a region of enhanced hole concentration, whereas in undoped samples the rest of the crystal is depleted of holes.

(3) The mobility of the holes is smaller in the disturbed regions around the dislocations than in the

material which is free of dislocations.

(4) Introduction of acceptors by doping (impurity atoms) or irradiation and quenching (vacancies) populates the dislocation-free regions of the samples with holes and results in an increase of the effective mobility.

(5) The dislocations (in duplex  $a$  deformed samples) cause acceptor levels 3 meV above the valence-band edge and the impurity atoms (antimony) 1 meV above, whereas the levels of the vacancies are located slightly below the valence-band edge. There is no donor action of the interstitials.

(6) In the 50-K recovery stage a correlated close-pair recombination occurs, whereas the recovery stage between 100 and 150 K is caused by an uncorrelated vacancy-interstitial recombination.

### ACKNOWLEDGMENTS

The authors would like to thank H. Roos and G. Freitag for experimental assistance and the Bundesministerium für Forschung und Technologie, Bonn, for sponsoring the project.

\*Based on a Ph.D. thesis submitted to the University of Würzburg, Germany.

- <sup>1</sup>E. Gmelin, R. Stapf, P. Klemt, G. Landwehr, W. Lichtenberg, and A. Przybylski, in *Radiation Effects in Semiconductors*, edited by J. W. Corbett and A. D. Watkins (Gordon and Breach, New York, 1971), p. 337.
- <sup>2</sup>E. Gmelin, R. Saffert, G. Landwehr, W. Lichtenberg, and P. Klemt, in *Radiation Damage and Defects in Semiconductors*, edited by J. E. Whitehouse (Institute of Physics, London, 1973), p. 394.
- <sup>3</sup>R. Saffert, E. Gmelin, and G. Landwehr, in *Lattice Defects in Semiconductors—1974*, edited by F. A. Huntley (Institute of Physics, London, 1975), p. 249.
- <sup>4</sup>R. Saffert, E. Gmelin, and G. Landwehr, *J. Phys. C* **11**, 2711 (1978).
- <sup>5</sup>M. Roos, Diplomarbeit, University of Würzburg, 1975 (unpublished).
- <sup>6</sup>T. Englert, K. von Klitzing, R. Silbermann, and G. Landwehr, *Phys. Status Solidi B* **81**, 119 (1977).
- <sup>7</sup>J. di Persio, J. C. Doukhan, and G. Saada, *Phys. Status Solidi* **42**, 281 (1970); **42**, 297 (1970).
- <sup>8</sup>J. C. Doukhan and B. Escaig, *Phys. Status Solidi A* **7**, 441 (1971).
- <sup>9</sup>D. A. Abokarov, E. Y. Banyulis, G. B. Bagdjev, G. A. Ivanov, N. G. Polikhronidi, and V. I. Chernobai, *Fiz. Tekh. Poluprovodn.* **7**, 579 (1973).
- <sup>10</sup>U. von Alpen, J. C. Doukhan, B. Escaig, and P. Grosse, *Phys. Status Solidi B* **55**, 667 (1973).

- <sup>11</sup>U. von Alpen, Thesis, Technische Hochschule Aachen, 1973 (unpublished).
- <sup>12</sup>J. C. Doukhan, R. Drope, J. L. Farvacque, E. Gerlach, and P. Grosse, *Phys. Status Solidi B* **64**, 237 (1974).
- <sup>13</sup>G. Faivre, *Philos. Mag.* **29**, 1289 (1974).
- <sup>14</sup>S. A. Abakarov, R. A. Amirova, and G. B. Bagdjev, *Fiz. Tverd. Tela (Leningrad)* **20**, 649 (1978).
- <sup>15</sup>K.-H. Landeck, G. Freitag, K. Keck, and A. Kühnel, in *Defects and Radiation Effects in Semiconductors—1978*, edited by J. H. Albany (Institute of Physics, London, 1979), p. 433.
- <sup>16</sup>P. Grosse, *Die Festkörpereigenschaften von Tellur*, Vol. 48 of *Springer Tracts in Modern Physics* (Springer, Berlin, 1969).
- <sup>17</sup>E. Schmid and W. Boas, *Kristallplastizität*, Vol. 17 of *Struktur und Eigenschaften der Materie* (Springer, Berlin, 1935).
- <sup>18</sup>J. Vogler, *Phys. Rev.* **79**, 1023 (1950).
- <sup>19</sup>R. Saffert, J. Schapawalow, G. Landwehr, and E. Gmelin, *Phys. Status Solidi B* **61**, 509 (1974).
- <sup>20</sup>O. Madelung, *Elektrische Leitungsphänomene II*, Vol. 20 of *Handbuch der Physik* (Springer, Berlin, 1957).
- <sup>21</sup>E. Bangert, D. Fischer, and P. Grosse, *Phys. Status Solidi B* **55**, 527 (1973); **59**, 419 (1973).
- <sup>22</sup>D. Thanh, *Solid State Commun.* **9**, 631 (1971).
- <sup>23</sup>K.-H. Helmreich, Thesis, University of Würzburg, 1979 (unpublished).
- <sup>24</sup>K.-H. Helmreich, K. Keck, G. Landwehr, and H. Roos, Proceedings of the International Conference on

- Radiation Physics of Semiconductors and Related Materials, Tbilisi, USSR, 1979, in press.
- <sup>25</sup>G. Landwehr, in *Radiation Effects in Semiconductors 1976*, edited by N. B. Urli and J. W. Corbett (Institute of Physics, London, 1977), p. 112.
- <sup>26</sup>C. Weigel, G. Landwehr, and J. W. Corbett, in *Lattice Defects in Semiconductors 1974*, Ref. 3, p. 241.
- <sup>27</sup>A. Koma and S. Tanaka, in *Radiation Damage and Defects in Semiconductors*, Ref. 2, p. 402.
- <sup>28</sup>K. Takita, T. Hagiwara, and S. Tanaka, *J. Phys. Soc. Jpn.* 31, 1469 (1971).
- <sup>29</sup>H. R uthlein, Diplomarbeit, University of W urzburg, 1975 (unpublished).
- <sup>30</sup>R. Saffert, Thesis, University of W urzburg, 1973 (unpublished).
- <sup>31</sup>K.-H. Helmreich, G. Freitag, K. Keck, G. Landwehr, and H. Roos, in *Defects and Radiation Effects in Semiconductors 1978*, Ref. 15, p. 440.
- <sup>32</sup>V. Heine, *Phys. Rev.* 146, 568 (1966).
- <sup>33</sup>R. A. Brown, *Phys. Rev.* 156, 889 (1967).
- <sup>34</sup>H. Teichler, in *Lattice Defects in Semiconductors 1974*, Ref. 3, p. 374.
- <sup>35</sup>K. von Klitzing and C. R. Becker, *Solid State Commun.* 20, 147 (1976).